Ab initio characterization of the Ne–I2 van der Waals complex: Intermolecular potentials and vibrational bound states

Laura Delgado-Tellez, Álvaro Valdés, Rita Prosmiti, Pablo Villarreal, and Gerardo Delgado-Barrio

Citation: J. Chem. Phys. **134**, 214304 (2011); doi: 10.1063/1.3596604
View online: http://dx.doi.org/10.1063/1.3596604
View Table of Contents: http://jcp.aip.org/resource/1/JCPSA6/v134/i21
Published by the American Institute of Physics.

Ab initio characterization of the Ne–I_2 van der Waals complex: Intermolecular potentials and vibrational bound states

Laura Delgado-Tellez, Álvaro Valdés, Rita Prosmiti,[a] Pablo Villarreal, and Gerardo Delgado-Barrio
Instituto de Física Fundamental (IFF-CSIC), CSIC, Serrano 123, 28006 Madrid, Spain and Hospital del Henares, 28820 Coslada, Madrid, Spain

(Received 13 April 2011; accepted 13 May 2011; published online 6 June 2011)

A theoretical study of the potential energy surface and bound states is performed for the ground state of the NeI_2 van der Waals (vdW) complex. The three-dimensional interaction energies are obtained from *ab initio* coupled-cluster, coupled-cluster single double (triple)/complete basis set, calculations using large basis sets, of quadruple- through quintuple-zeta quality, in conjunction with relativistic effective core potentials for the heavy iodine atoms. For the analytical representation of the surface two different schemes, based on fitting and interpolation surface generation techniques, are employed. The surface shows a double-minimum topology for linear and T-shaped configurations. Full variational quantum mechanical calculations are carried out using the model surfaces, and the vibrationally averaged structures and energetics for the NeI_2 isomers are determined. The accuracy of the potential energy surfaces is validated by a comparison between the present results and the corresponding experimental data available. In lieu of more experimental measurements, we also report our results/predictions on higher bound vibrational vdW levels, and the influence of the employed surface on them is discussed. © *2011 American Institute of Physics*. [doi:10.1063/1.3596604]

I. INTRODUCTION

One of the major motivation for research on rare gas(Rg)-halogen van der Waals (vdW) complexes is to better understand long-range intermolecular forces and energy transfer mechanisms. For this reason many combinations of a rare gas atom with a halogen molecule have been studied by both theory and experiment (see Refs. 1–5 and references therein). On the one hand, the apparent simplicity of these systems has attracted the attention of theoreticians,[4,6–10] however, one of the primary difficulties encountered in theoretical treatments is posed by the lack of accurate data for the intermolecular potential energy surfaces (PESs). Nowadays, *ab initio* methods have been readily applied to such weak complexes, and potential energy surfaces have been derived from high-level electronic structure calculations for the ground and excited states.[5,11–17] These potentials have predicted the coexistence for both linear and T-shaped isomers for the X-state Rg-dihalogen complexes, with the linear one being the most stable for most of them.[5,18–21]

On the other hand, recent experimental observations from laser-induced-fluorescence, action, and two-laser pump-probe spectroscopy techniques have stabilized ground-state complexes, and X → B spectra of a variety of linear Rg-dihalogen complexes have been reported.[1,4,10,22] Further, from these experiments the binding energies of the two isomers have been measured, and, in general, a good agreement with the theoretical predicted values has been found, with the ground state linear isomer to be energetically more stable than the T-shaped one, except the case of He–I_2.[4,5,23] Based upon this agreement between theory and experiment, we have chosen to further interrogate the Ne–I_2 cluster, aiming to advance in our understanding of Rg-dihalogen ground state interactions.

A key point for carrying out a reliable study is the description of the underlying potential energy surface. So far, recently MP2 and coupled-cluster single double (triple) [CCSD(T)] *ab initio* calculations have been reported in the literature[24] at only the linear and T-shaped geometries, and until now no *ab initio* intermolecular potentials exist for the NeI_2 complex. However, data on binding energy are available for both ground and excited B states of the Ne–I_2 complex from the early experimental studies by Levy and co-workers.[25] In particular from these experiments, energy D_0 values of 72.4–74.7 and 65.0–67.1 cm^{-1} have been determined for the X and B states, respectively. Later on experimental observations on this complex[26] have provided new binding energy values of 65.3 ± 1.0 and 57.6 ± 1.0 cm^{-1} for its X and B state, respectively. Further, these studies have indicated that the average geometry of the zero-point level of the Ne–I_2(X) is slightly delocalized, sampling mainly T-shaped configurations of the complex, and with appreciable amplitude for the linear ones. However, they have concluded that it is improbable that there are two dynamically stable isomers for the ground Ne–I_2 cluster. The spectroscopy and dynamics of this complex have also been studied employing pairwise additive vdW potential, and more recently the first-order diatomics-in-molecules perturbation theory (DIM-PT1) method has been applied to construct an intermolecular PES for Ne–I_2.[27] These DIM-PT1 surfaces have been constructed taking into account the double-minimum topology for both Ne–I_2(X and B) states, and with the ground T-shaped well-depth being 74.7 cm^{-1}, while the corresponding linear

[a]Electronic mail: rita@iff.csic.es.

well is 52.6 cm^{-1}. As we mentioned before, recently MP2 and CCSD(T) calculations have been carried out, and well-depths between 82.4–117.1 cm^{-1} and 81.2–89.7 cm^{-1} have been reported for the linear and T-shaped geometries of the NeI_2 ground state complex, respectively.[24] Unfortunately, no more data are available in the literature for this vdW complex.

Thus, the results presented here are motivated by a desire to characterize, based on high level of *ab initio* calculations, the potential surface of the ground Ne–I_2. We aim to provide insight into how the ground intermolecular potential surface is affected in going from He to Ne, and the effect of this change on the relative stability of the linear and T-shaped isomers obtained from quantum variational bound state calculations of the whole system. Such results could also be helpful in understanding the difference in the relative stability of the ground state He–I_2 isomers that are observed experimentally,[4] and to discuss general trends in the whole set of such complexes.[5,20] Further, based on accurate PESs of the triatomic species, realistic potential energy surfaces of larger clusters, Rg_n-dihalogen could be constructed in order to study their spectroscopy, gas-phase solvation effects, and/or photodynamics of size-selected species.[28–32]

The plan of this paper is as follows: Sec. II describes the computational details together with the results obtained from *ab initio* electronic structure calculations. In addition, the generation of potential energy surfaces, such as an analytical parametrized model surface to *ab initio* data, and the one constructed by an interpolation process is described. At the end, quantum vibrational bound state computations, and their comparison with the experimental data available are also presented. A summary and some conclusions constitute Sec. III.

II. COMPUTATIONAL METHODS AND RESULTS

A. Details of *ab initio* calculations

The calculations are carried out using the MOLPRO package.[33] We employ the spin-restricted single and double excitations coupled cluster method with perturbative triples [RCCSD(T)] in the supermolecular approach. The basis set superposition error was corrected by the counterpoise method[34] for each molecular configuration. We use Jacobi coordinates (r, R, θ) to describe the potential surface of NeI_2 complex, where R is the intermolecular distance of Ne atom from the center of mass of I_2, r is the bond length of I_2, and θ is the angle between the **R** and **r** vectors.

Scalar relativistic effects were accounted for by using relativistic effective core potentials (ECPs) for the I atoms. Results obtained using large-core potentials, denoted by ECP46MWB (Ref. 35) and ECP46MDF,[36] in conjunction with their associated basis sets,[36,37] are compared with the ones from the small-core potential, denoted by ECP28MDF (Ref. 38) calculations using the augmented correlation consistent basis sets aug-cc-pVQZ-PP and aug-cc-pV5Z-PP optimized by Peterson *et al.*[38] In the large-core calculations core-valence correlation effects were accounted for by using core polarization potentials, while core-core and core-valence correlation effects were entirely neglected in the small-core calculations. For Ne atom, the corresponding aug-cc-pV(Q/5)Z basis sets were used.

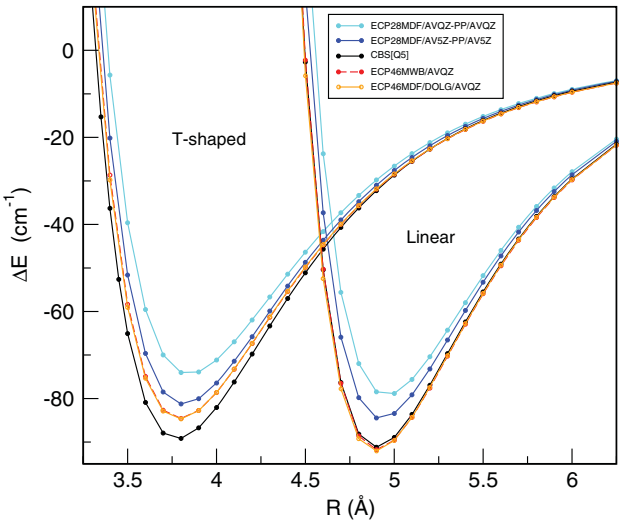

FIG. 1. CCSD(T) and CBS[Q5] interaction energies for linear and T-shaped configurations for $r = 2.666$ Å using the indicated ECPs and basis sets.

Figure 1 shows a comparison of RCCSD(T) interaction energies for small and large ECPs with different basis sets. For the small-core ECPs a series of correlation consistent basis sets are available, and this allows to extrapolate the energies to the (approximate) complete basis set (CBS) limit. We performed extrapolation of the correlation energies utilizing the two-point single inverse power function first introduced by Schwartz,[39] $E_X = E_{CBS} + A/X^3$, assuming the aug-cc-pVXZ, with X = Q and 5, basis sets. One can see that using large-core ECPs we obtained lower interaction energies than with the small-core ones. In particular, the CBS[Q5] interaction energies compare pretty well with the values obtained from the large-core calculations. The CBS[Q5] values are found to be somehow slightly higher for the linear geometries, while for the T-shaped configurations differences for both repulsive and attractive parts of the curve are obtained. Based on these comparisons, as well as the better CCSD(T)

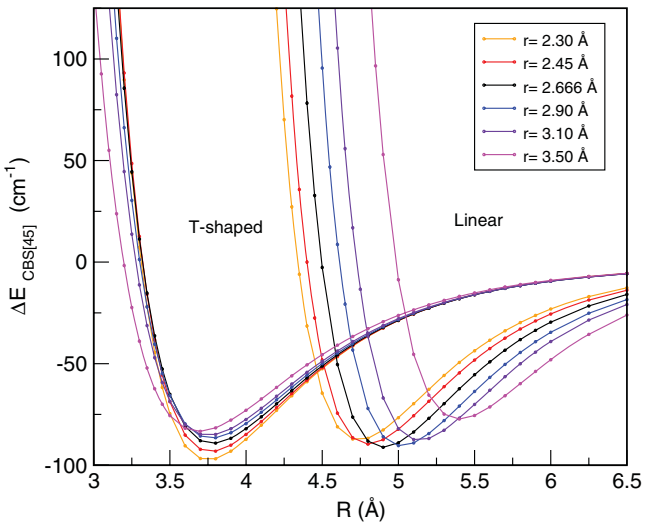

FIG. 2. CBS[Q5] interaction energies for the linear and T-shaped configurations as a function of r bond distance.

TABLE I. Parameters for the $V(R,\theta_j;r_k)_{j=1-7,k=1-5}$ potential, (Eq. (2)) for NeI_2 complex. σ^{jk} is the partial averaged standard deviation for each θ_j and r_k values. Distances are in Å and energies in cm^{-1}. Figures in parentheses are powers of 10.

			$r = 2.30$ Å			
θ(deg)	α_0^{j1}	α_1^{j1}	α_2^{j1}	α_3^{j1}	α_4^{j1}	σ^{j1}
0	173.824	1.8267	4.47097	1.39095(06)	−4.65276(07)	0.3062
15	158.934	1.78131	4.48904	1.33788(06)	−4.67316(07)	0.2587
30	228.386	1.70709	4.29457	1.40755(06)	−5.9653(07)	0.2603
45	0.0290229	1.58007	7.15093	38295.8	2.58279(07)	0.2766
60	0.00298049	1.53287	7.7605	119746	1.68924(07)	0.2491
75	0.00889258	1.56687	7.01879	239189	7.99529(06)	0.1737
90	0.00440543	1.63435	6.9144	271940	5.26741(06)	0.1737
			$r = 2.45$ Å			
θ	α_0^{j2}	α_1^{j2}	α_2^{j2}	α_3^{j2}	α_4^{j2}	σ^{j2}
0	183.128	1.81845	4.52698	1.53326(06)	−5.37321(07)	0.3313
15	172.105	1.77232	4.53472	1.48023(06)	−5.48449(07)	0.3132
30	263.441	1.70133	4.30653	1.59103(06)	−7.14383(07)	0.3149
45	0.909301	1.58001	6.08535	82624.7	2.29213(07)	0.3279
60	0.0434275	1.52446	6.92076	117322	1.73016(07)	0.2871
75	0.0193135	1.54647	6.82574	235054	8.32499(06)	0.1937
90	0.0161707	1.60739	6.57044	281684	5.04102(06)	0.1744
			$r = 2.666$ Å			
θ	α_0^{j3}	α_1^{j3}	α_2^{j3}	α_3^{j3}	α_4^{j3}	σ^{j3}
0	161.553	1.80508	4.67123	1.60491(06)	−5.57336(07)	0.3179
15	166.987	1.75744	4.64862	1.62232(06)	−6.23034(07)	0.2975
30	245.751	1.68831	4.42118	1.70904(06)	−7.88589(07)	0.2660
45	2.83545	1.57035	5.7815	103749	2.14981(07)	0.3406
60	0.0496247	1.50238	6.95699	77929.8	1.97378(07)	0.3188
75	0.0114288	1.51962	7.06772	235402	8.73127(06)	0.1898
90	0.00365298	1.57496	7.10362	298385	4.75624(06)	0.1298
			$r = 2.90$ Å			
θ	α_0^{j4}	α_1^{j4}	α_2^{j4}	α_3^{j4}	σ^{j4}	
0	162.734	1.78467	4.79153	1.8197(06)	−6.75523(07)	0.3374
15	183.339	1.73604	4.73779	1.90446(06)	−8.05202(07)	0.3140
30	374.669	1.67035	4.37147	2.26275(06)	−1.18924(08)	0.3419
45	0.0326247	1.54306	7.34531	−122 971	3.91605(07)	0.3764
60	0.0266302	1.47596	7.26155	26 409.6	2.29711(07)	0.3647
75	0.00211437	1.49281	7.70182	237 758	9.05437(06)	0.1842
90	0.0197231	1.54414	6.61209	315 800	4.13142(06)	0.1217
			$r = 3.10$ Å			
θ	α_0^{j5}	α_1^{j5}	α_2^{j5}	α_3^{j5}	α_4^{j5}	σ^{j5}
0	113.971	1.77269	5.00424	1.65074(06)	−5.38237(07)	0.2539
15	183.469	1.71671	4.8415	2.10503(06)	−9.47242(07)	0.3226
30	336.727	1.65371	4.49392	2.37018(06)	−1.28192(08)	0.3320
45	0.043176	1.52646	7.33926	−185376	4.41574(07)	0.4061
60	0.00532763	1.458	7.87866	13023	2.48385(07)	0.3576
75	0.00671159	1.47185	7.36351	244658	8.87129(06)	0.1760
90	0.051015	1.52056	6.32362	329171	3.49905(06)	0.1235

results obtained for the I_2 spectroscopic constants,[16] we decided to perform the final calculations using the small-core ECP28MDF pseudopotentials together with the aug-cc-pVQ/5Z-PP basis sets for the I atoms,[38] and the aug-cc-pVQ/5Z basis sets for the Ne atoms. The interaction energies, CCSD(T)/CBS[Q5], are then obtained, as we mentioned above, by applying the two-point extrapolation scheme.[39]

The intermolecular energies are calculated for R distances ranging from $R = 2.7$ to 11 Å, while the angle θ is varied between 0° and 90° on seven equally spaced (by 15°) grid, considering six different I_2 bond-lengths with $r = 2.30$, 2.45, 2.666, 2.90, 3.10, and 3.50 Å. The total grid consists of 1653 configurations.

In Fig. 2, we plot the *ab initio* CBS[Q5] interaction energies for $\theta = 0°$ and 90°, and for all the r values studied. As can be seen, the interaction for the T-shaped configurations is predicted to become less attractive as r increases, while the interaction at linear configurations is much less affected, with these configurations to be displaced at larger intermolecular distances R.

B. Generation of the potential energy surface

For representing the potential energy surface for the NeI_2 complex we used two different schemes: one based on a fitting procedure and another one on an interpolation process within the reproducing kernel Hilbert space (RKHS) method by Ho and Rabitz.[40]

In the first case, as in our previous studies on such complexes,[21,23] we employ an expansion in Legendre polynomials,

$$V(R,\theta;r_k) = \sum_{\lambda} V_{\lambda}^{k}(R) P_{\lambda}(\cos\theta) \tag{1}$$

with $k = 1-6$ and $\lambda = 0, 2, 4, 6, 8$ to represent the PES. The $V_{\lambda}^{k}(R)$ coefficients are obtained by a collocation method, by fitting the CCSD(T)/CBS[Q5] *ab initio* data to a combined Morse+vdW function,

$$V(R;\theta_j;r_k) = \alpha_0^{jk}\left(\exp\left(-2\alpha_1^{jk}(R-\alpha_2^{jk})\right) - 2\exp\left(-\alpha_1^{jk}\left(R-\alpha_2^{jk}\right)\right)\right) - \frac{\alpha_3^{jk}}{R^6} - \frac{\alpha_4^{jk}}{R^8}, \tag{2}$$

using a nonlinear least square technique. The five adjusted parameters $\alpha_{p=0-4}^{jk}$ are listed in Table I together with the corresponding partial average standard deviation for each angle value. We show that for $r = 3.50$ Å the parametrized PES presents some convergence problems for angular θ values between 77° and 88°, and thus further on we include only the five r values for the analytical representation of the surface. For all calculated grid points we found a total average standard deviation of 0.272 cm^{-1} with a maximum standard deviation of 0.471 cm^{-1}. The parametrized potential represents very well the *ab initio* data, and, in particular, the T-shaped and near T-shaped configurations (see Table I).

In the second one, we follow a procedure based on the RKHS method[40] writing the interaction energy as

$$V(R,\theta;r_k) = \sum_{i=1}^{N_R}\sum_{j=1}^{N_\theta} v_{ij}^{k} q_1^{2,5}(R_i,R) q_2(y_j,y), \tag{3}$$

where $y = \cos\theta$, N_R and N_θ are the number of *ab initio* calculated points in each coordinate, $q_1^{n,m}$ and q_2 are the one-dimensional (1D) reproducing kernel functions for the distance-like, R, and angle-like, θ, variables, respectively.[40]

The expressions of these functions are

$$q_1^{n,m}(x,x') = n^2 x_>^{-(m+1)} B(m+1,n)\,{}_2F_1\left(-n+1, m+1; n+m+1; \frac{x_<}{x_>}\right), \tag{4}$$

$$q_2(y,y') = \sum_{l} \frac{(2l+1)}{2} P_l(y) P_l(y'), \tag{5}$$

where $x_>$ and $x_<$ are the larger and smaller of the x and x', respectively, n and m superscripts refer to the order of smoothness of the function and its asymptotic behavior at larger distances, B is the beta function, ${}_2F_1$ is the Gauss hypergeometric function,[40] and $l = 0, 2, 4, 6, 8$. The linear coefficients, v_{ij}^{k}, are obtained as the solutions of Eq. (3), where

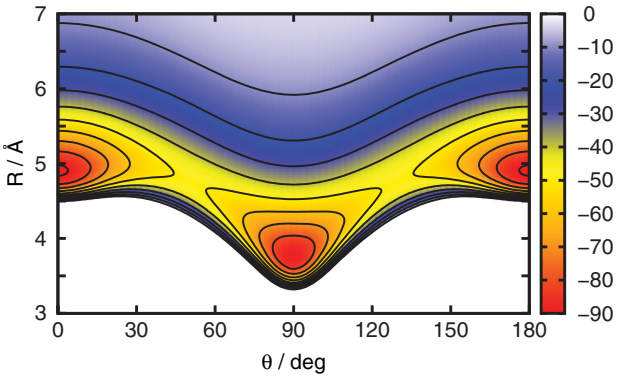

FIG. 3. Two-dimensional contour plot of the analytical potential surface of Eq. (1) of Ne–I_2(X) in the (θ, R)-plane. The bond distance of I_2 is fixed to 2.666 Å.

$V(R_i,\theta_j;r_k)$ is the *ab initio* CCSD(T)/CBS[Q5] calculated interaction energy at the corresponding $(R_i,\theta_j;r_k)$ grid point. For the three-dimensional representation of the PES, in both cases, an one-dimensional cubic spline interpolation is employed in the r coordinate.

In Fig. 3, a two-dimensional contour plot of the analytical NeI_2 PES (see Eq. (1)), for fixed $r = 2.666$ Å bond-length, is shown. The surface presents two minima for linear and T-shaped geometries, with very similar well-depths. In Fig. 4, we show the minimum energy path between the potential minima, obtained from the analytical parametrized surface (see Eq. (1)), in comparison with the calculated *ab initio* CCSD(T)/CBS interaction energies at the indicated geometries as a function of θ and r coordinates. One can see that for both surfaces, the model analytical surface and the one from the RKHS interpolation, the T-shaped minima are shifted to shorter r values ($r = 2.30$ Å) with a well-depth of 97.23 cm^{-1}, compared to 97.34 cm^{-1} from the RKHS one, while the linear one remains close to the I–I equilibrium distance. For this r value of 2.666 Å the linear potential minimum is at an energy of –91.31 cm^{-1} (–90.75 cm^{-1} from the

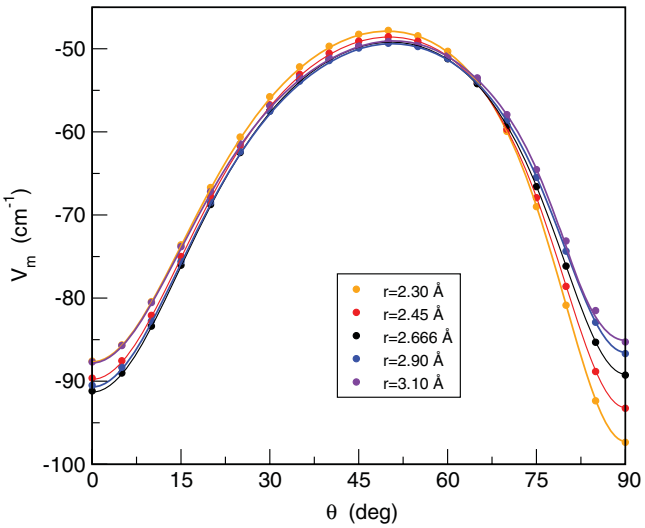

FIG. 4. Minimum energy values obtained from the parametrized potential together with the corresponding CCSD(T)/CBS[Q5] interaction energies as a function of θ and r.

RKHS) and $R = 4.90$ Å, while the T-shaped one has an energy of –89.14 cm^{-1} (–88.89 cm^{-1} from the RKHS PES) at $R = 3.78$ Å. The corresponding barrier between these two wells is found at an energy of about –49.21 cm^{-1} (–48.91 cm^{-1} from RKHS) at R = 4.77 Å and $\theta \sim 50^o$. The accuracy of the fit as well as the RKHS interpolation is checked by comparing with the CCSD(T)/CBS[Q5] *ab initio* points along the above mentioned minimum energy path (not included in both fitting and interpolation schemes). For these configurations we found an averaged deviation of 0.15 and 0.11 cm^{-1} for the analytical fitted and RKHS interpolated PESs, respectively.

As we mentioned above from a recent study[24] on NeI_2, well-depths of 82.4–117.1 cm^{-1} and 81.2–89.7 cm^{-1} have been estimated from the MP2 and CCSD(T) calculation of the linear and T-shaped geometry, respectively. In this latter work,[24] a wide range of the well-depth values, depending mainly of the basis set used, have been reported with the ones from the CCSD(T) calculation and with the larger basis set to predict a rather large difference of 21.3 cm^{-1} between the two potential wells. As there are no more previous *ab initio* studies on the NeI_2 cluster available in the literature, we can further compare only with a semiempirical surface based on a DIM-PT1 approach,[27] as well as with the early experimental estimates by Levy and co-workers.[25] The DIM-PT1 has predicted a T-shaped well-depth of 74.7 cm^{-1} as the global minimum of the ground Ne–I_2 surface, and a secondary minimum for a linear configuration, 11.9 cm^{-1} above it. From the experimental study[25] a well-depth in the range of 84.5–86.4 cm^{-1} for the T-shaped geometry has only been reported. As we can see, the present calculations are completely different from the previous estimates available in the literature on the linear potential well of this complex. However, for the T-shaped well a better accord is found with the recent *ab initio* study and the early experimental estimate, as well as with both theoretical and experimental investigations, on similar molecular systems.[4,5,20,22]

C. Quantum bound state calculations

As in our earlier studies,[5,21,23] the bound vdW levels and corresponding wave functions are calculated variationally by diagonalizing the vibrationally averaged Hamiltonian of the system.

$$H_v = \langle \chi_v | H | \chi_v \rangle = -\frac{\hbar^2}{2\mu_1}\frac{\partial^2}{\partial R^2} + \frac{\hat{l}^2}{2\mu_1 R^2} + V_{v,v}(R,\theta) + E_{I_2}(v) + \frac{B_v \hat{j}^2}{\hbar^2}, \quad (6)$$

where $E_{I_2}(v)$ and $\chi_v(r)$ are the eigenvalues and eigenfunctions of the diatomic $\hat{H}_{I_2}$ Hamiltonian obtained by solving the 1D Schrödinger equation using the I_2 ground state potential from Ref. 5. $\hat{l}$ and $\hat{j}$ are the angular momentum operators associated with the vectors **R** and **r**, respectively, leading to a total angular momentum $\hat{J} = \hat{l} + \hat{j}$. $V_{v,v}(R,\theta) = \langle \chi_v | V(R,\theta,r) | \chi_v \rangle$ is the intermolecular vdW potential of NeI_2 averaged over the I_2 $v = 0$ vibrational eigenfunction and B_v is the I_2 average rotational constant. In Fig. 5, we plot the minimum energy path of the vibrationally $V_{0,0}$ averaged potentials obtained from the fitting and RKHS procedures. As we can see both curves are very similar to each other, with some small differences around the linear well and isomerization barrier, and somehow more pronounced ones nearby the T-shaped well. As we will discuss below, these discrepancies in the potential representation will influence the properties of the vibrational states of the NeI_2 system.

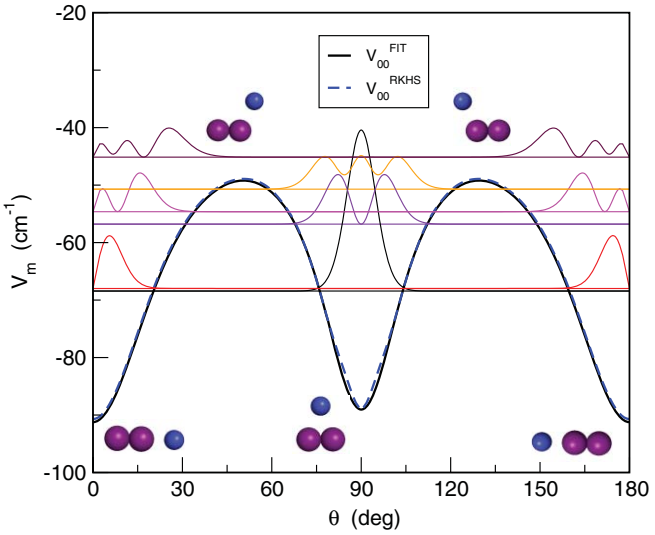

FIG. 5. Minimum energy path of the vibrationally averaged potentials $V_{v,v}$ of the Ne–I_2(X,$v = 0$) as a function of angle θ obtained for the analytical fit from Eq. (1), and for the RKHS interpolation from Eq. (3). The energies and angular probability distributions of the 8 lowest intermolecular vdW levels for $J = 0$ of the RKHS PES are also superimposed. For each eigenstate the zero probability value is shifted to its energy value given in Table II.

The Hamiltonian is represented on a finite three-dimensional basis set: in R coordinate, 140 DVR particle-in-box functions over the range from $R = 2.85$ to 12.0 Å are used, in θ we used orthonormalized Legendre polynomials $\{P_j(\cos\theta)\}$ as basis functions, with a total of 80 values of the diatomic rotation j, for both even and odd symmetry. In the r coordinate, we use 61-points Gaussian quadrature in the range of 2.2–3.4 Å, and it is then diagonalized, achieving a convergence of 10^{-6} in the bound state energies.

In Table II we list the lowest nine vibrational energies of the NeI_2(X,$v = 0$) vdW states for $J = 0$, for both analytical and RKHS PESs. In Fig. 5, we plot the angular probability distributions of these states calculated with the RKHS PES, while in Figs. 6 and 7 we display bidimensional D(θ,R) probability distributions of them for the RKHS and analytical model PES, respectively. The zero-point $n = 0$ vibrational level is found at energy of –69.62 and –68.43 cm^{-1} for the parametrized and RKHS surface, respectively, and as we can see in Figs. 5, 6, and 7 that its associated eigenfunction corresponds to T-shaped isomer with an averaged R_0 value of 3.91/3.93 Å for the analytical/RKHS PES. The next two vibrational states, $n = 1$ (even) and 2 (odd), at energy of –68.56 and –67.98 cm^{-1} for analytical and RKHS surfaces, respectively, are predicted to be a degenerate pair of levels and are localized at linear configurations with $R_0 = 5.01/5.02$ Å. We found that the energy difference between the degenerate pair and the ground vdW state is very small, of 1.05 and 0.45 cm^{-1} for the analytical and RKHS PES,

TABLE II. Energies for the indicated vibrational vdW level of $NeI_2(X)$.

	This work ($v = 0$)			
n	Analytic/FIT PES	RKHS PES	DIM-PT1 PES (see Ref. 27)	Expt. (see Refs. 26 and 41)
0	−69.618	−68.432	−58.454	65.3 ± 1.0
1	−68.564	−67.980	−49.649	72 ± 3
2	−68.564	−67.980	−43.680	
3	−58.010	−56.787	−38.805	
4	−55.150	−54.634	−38.805	
5	−55.150	−54.634	...	
6	−51.254	−50.713	...	
7	−45.750	−45.134	...	
8	−45.599	−45.134	...	

respectively, indicating the coexistence of two dynamically stable isomers of $Ne–I_2(X)$ at very low temperatures. We should note that the predicted energy difference between the two isomers is larger for the analytical model surface than the RKHS one. As we mentioned before, there are some differences in the present potential surfaces, small ones for the linear well and larger for the T-shaped one. One can see in Fig. 5 and Table III that the linear well is by 0.52 cm^{-1} deeper for the analytical surface than the RKHS one, while the well-depth value for the T-shaped one is smaller for the RKHS one

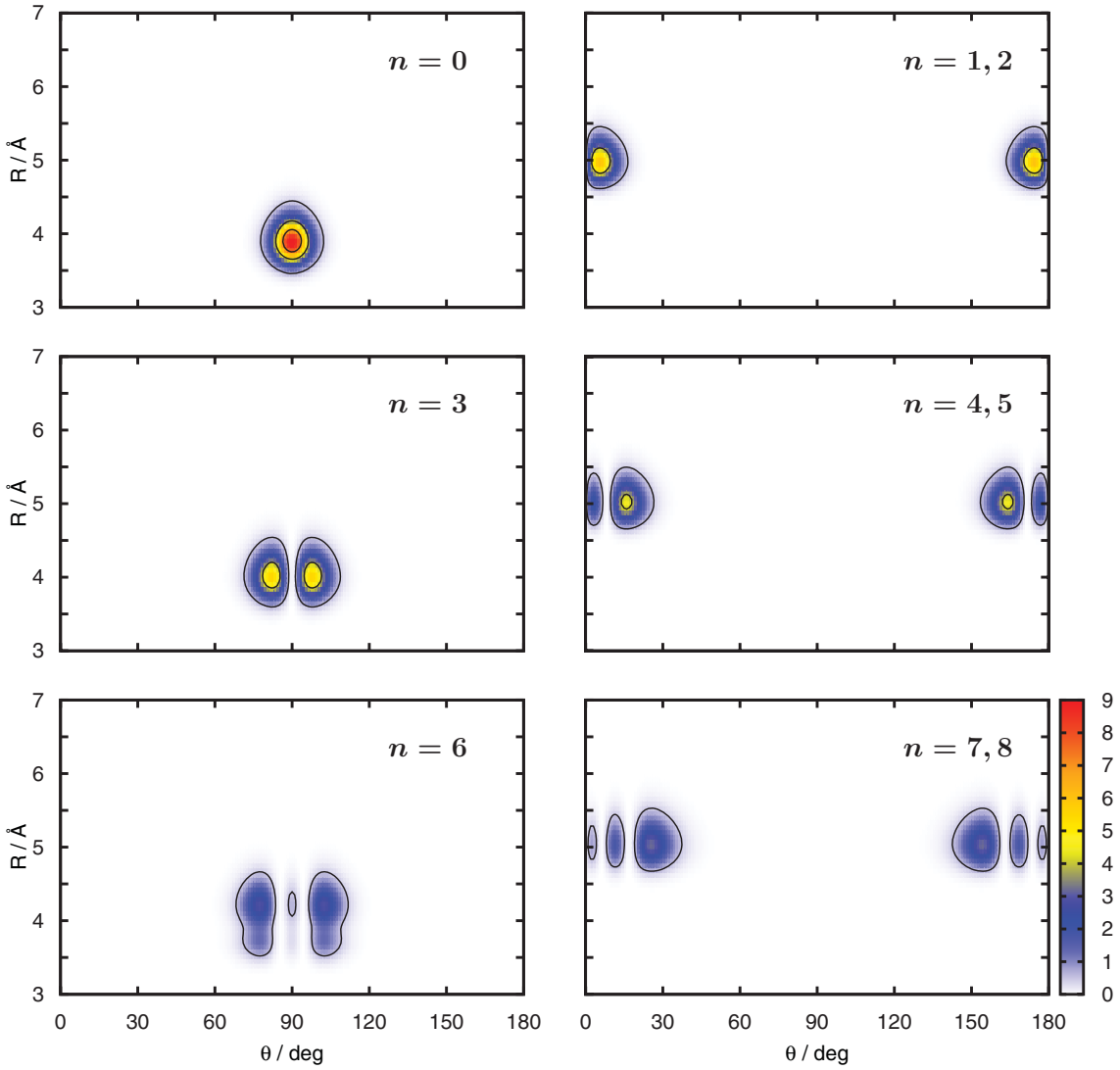

FIG. 6. Contour plots of the probability density distributions for the indicated vdW levels calculated using the RKHS PES of Eq. (3) for the $Ne–I_2(X,v = 0)$ complex.

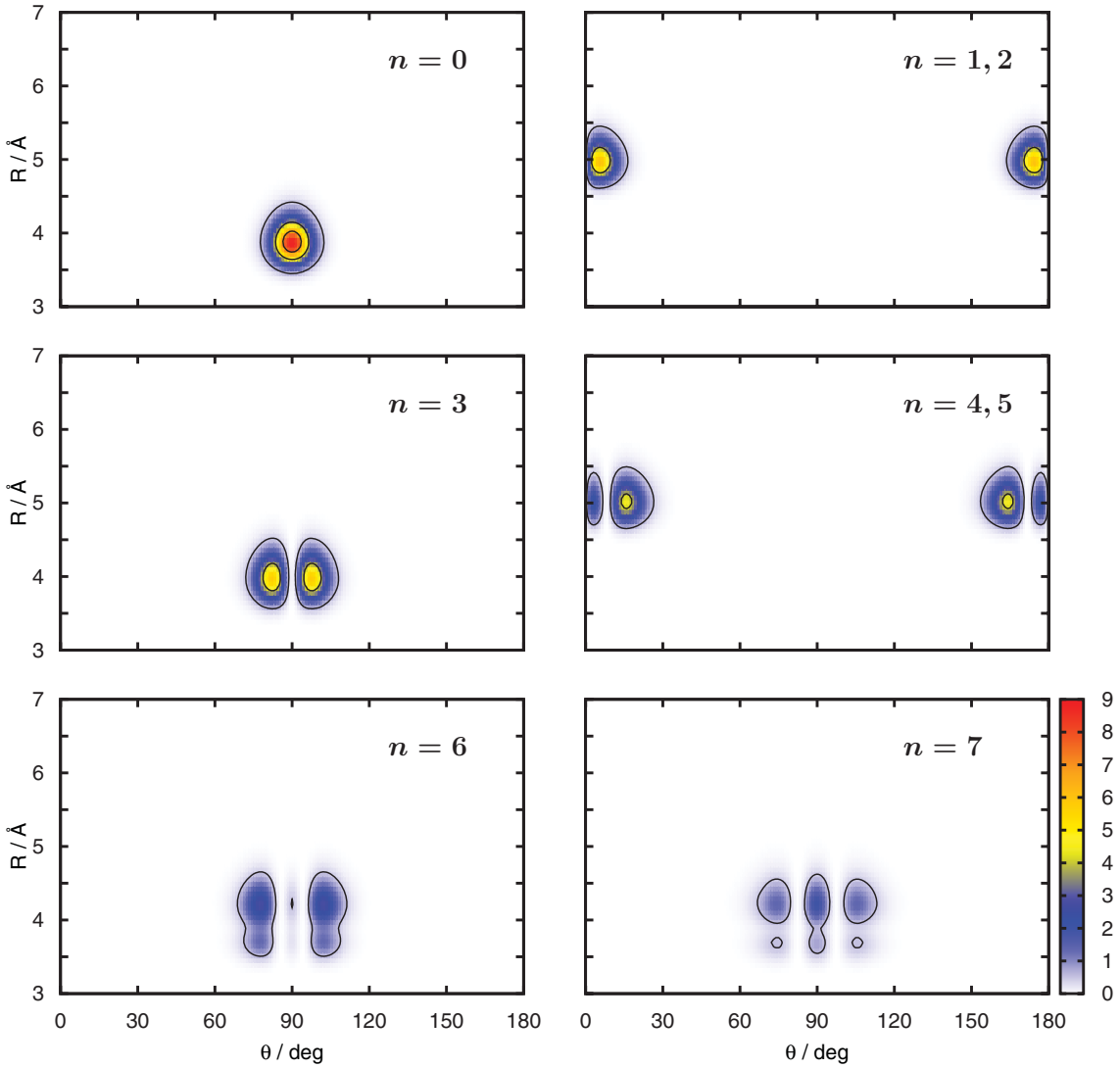

FIG. 7. Same as Fig. 6 using the analytical model PES of Eq. (1) for the Ne–I_2(X,$v = 0$) complex.

by 0.23 cm^{-1}, although this T-shaped well appears to be less anharmonic than one of the analytical model surface. Such differences are clearly reflected in the energy of these lowest, $n = 0$, 1, and 2, vibrational levels, while their corresponding eigenfunctions are not affected (see Figs. 6 and 7).

More vibrational states are also computed, and as we can see the next $n = 3$ one is lying 10.5 and 11.2 cm^{-1} higher in energy than the $n = 0$ for the analytical and RKHS surface, respectively, and up to the $n = 6$ state for both PESs there is a similar order of levels. We could easily assign them to bending and stretching excitations of the T-shaped ($n = 3$ and 6) or linear ($n = 4$ and 5) conformers, and anharmonic frequencies for the bending mode of 11.6 and 13.5 cm^{-1} for the T-shaped and linear wells, respectively, (see Table II and Figs. 6 and 7) are calculated. Contrary for the $n = 7$ state we found a different assignment for each PES. In particular, for the RKHS

TABLE III. Binding energies (D_e and D_0 in cm^{-1}), isomerization barrier, equilibrium, and vibrationally averaged distances (in Å) of the Ne–I_2(X, $v = 0$) complex.

NeI_2	Linear		Barrier	T-shaped	
	D_e/D_0	R_e/R_0	$E^*/(R,\theta)$	D_e/D_0	R_e/R_0
CBS[Q5]/FIT PES ($v = 0$)	91.22/68.56	4.91/5.01	–49.21/(4.77,50.3)	89.04/69.62	3.78/3.91
CBS[Q5]/RKHS PES ($v = 0$)	90.70/67.98	4.91/5.02	–49.01/(4.72,52.7)	88.81/68.43	3.78/3.93
MP2/CCSD(T) (see Ref. 24)	82.3–117.1/74.3–109.5	4.87–5.03/–	…	81.2–89.7/73.1–80.7	3.77–3.87/-
DIM-PT1 PES ($v = 0$) (see Ref. 27)	52.6/38.8	∼5.0/–	∼–38.0/∼(5.2,40.0)	74.7/58.5	∼4.1/-
Experiment (see Ref. 25)	…	…	…	84.5–86.4/72.4–74.7	…
Experiment (see Ref. 26)	…	…	…	–/64.3–66.3	…
Experiment (see Ref. 41)	–/72 ± 3.0	…	…	–/65.3 ± 1.0	…

surface the $n = 7$ and 8 states correspond to a degenerate pair of levels at an energy of –45.134 cm^{-1} assigned to the bending mode excitations of the linear isomer (see Fig. 6), while for the analytical model PES the $n = 7$ state is lying at an energy of –45.75 cm^{-1} and corresponds to a bending-stretching overtone of the T-shaped isomer (see Fig. 7), and the $n = 8$ is found by 0.15 cm^{-1} higher in energy, and is assigned, as in the RKHS surface (see Fig. 6), to the bending excitations of the linear isomer. We should mention that these states are at energies just above the potential isomerization barrier between the linear and T-shaped wells, and its higher value by 0.2 cm^{-1} in the RKHS case (see Table III) seems to influence their behavior.

In Table III, we compare the results obtained for the present CCSD(T)/CBS[Q5] surfaces with previous theoretical and experimental data available. The first experimental value for the $NeI_2(X)$ binding energy has been determined[25] to be between 72.4 and 74.7 cm^{-1}, while, later on, its value has been restricted between 64.3 and 66.3 cm^{-1},[26] and more recently a value of 65.3 ± 1.0 cm^{-1} has been obtained.[41] In both earlier experiments only the T-shaped isomers for the ground NeI_2 complex have been assigned, while recently experimental transitions of linear isomer have been observed, and an estimate of 72 ± 3 cm^{-1} has been obtained for its binding energy.[41] Our present estimates for the binding energies of the T-shaped and linear conformers show that the T-shaped one is slightly more stable, with a D_0 value of 69.62 and 68.43 cm^{-1}, (very close to each other) for the analytical and RKHS PESs, respectively. One can see that these values are very near to the lower bound of the later experimental values.[26,41] By comparing now the present prediction for the linear binding energy, we obtained a value of 68.56 and 67.98 cm^{-1} for the analytical and RKHS PES, respectively, that are close to the lower limit of the recent experimental one,[41] however, a different order of stability is found here for the two conformers. We should note that the predicted binding energies calculated here are for zero temperature of the system, while the experimental measurements have been obtained at temperatures of 0.5–5 K. Therefore, a part of the difference from the experimental energies could be attributed to the rotational excitation of the complex.

Further comparison with previous theoretical studies is also listed in Table III. The recent study of Ref. 24, based on a force-field analysis for the linear and T-shaped wells at MP2 and CCSD(T) levels of theory, has predicted a wide range of D_0 values, with one of their best calculation to count 101.6 and 80.3 cm^{-1} for the linear and T-shaped isomer, respectively. This finding indicates the failure of such analysis for highly coupled anharmonic systems and the need of full quantum treatments. Also, the results on binding energies from the semiempirical DIM-PT1 surface are shown, where completely different values of 58.5 and 38.8 cm^{-1} have been reported for the T-shaped and linear isomers of the $NeI_2(X, v = 0)$ cluster. One can see that the semiempirical surface was unable to describe quantitatively the intermolecular interactions for this complex.

By comparing now with previous theoretical results for the lighter HeI_2 cluster,[5] as it was expected, the interaction energies, as well as the binding energy values of the NeI_2 isomers are much larger. For both systems the linear well is deeper than the T-shaped one; however, the relative stability of their corresponding isomers is in reverse ordering, with a very small energy difference between these conformers of about 1% of their binding energies. In particular, for HeI_2 this energy difference counts for 0.2 cm^{-1} with the linear one to be slightly more stable, at energy of –15.72 cm^{-1}, than the T-shaped one and 1.05/0.45 cm^{-1} for the analytical/RKHS NeI_2 surfaces, with the T-shaped isomer to be more favored. As we can see, some general trends for the intermolecular interactions of the linear and T-shaped structures of such complexes are clear; however, anharmonic zero-point quantum effects are important, and full-dimensional quantum treatments using accurate PESs are needed for providing theoretical reliable results on their corresponding isomers.

III. SUMMARY AND CONCLUSIONS

We carried out a theoretical investigation on the NeI_2 van der Waals cluster. The full-dimensional intermolecular potential for the $Ne–I_2(X)$ complex is constructed from a grid of 1653 configurations. The *ab initio* calculations are performed using the CCSD(T) method and ECPs together with large consistent correlated basis sets at the CBS[Q5] limit. An analytic representation for the interaction potential is implemented based on two generation surface schemes. One is a fitting procedure of the *ab initio* interaction energies to a combined Morse+vdW functional form, while the other one is an interpolation method based on the RKHS approach.[40] The topology of the surface is investigated and two minima corresponding to linear Ne–I–I (global minimum) and T-shaped $Ne–I_2$ (local minimum) configurations are located.

The accuracy of the PESs is validated by comparing the theoretical values with the experimental measurements available on binding energies and average structures. Therefore, variational bound-state calculations are performed to compute the vdW states of the ground NeI_2 cluster using both surfaces. Contrary to our previous studies on HeI_2 (Ref. 5) and ArI_2 (Ref. 20) complexes, we found that for the ground state NeI_2 system the T-shaped isomer is more strongly bound than its linear counterpart. The binding energy of the T-shaped $Ne–I_2$ conformer is found to be 69.62 and 68.43 cm^{-1}, for the analytical and RKHS PES, respectively, while for the linear Ne–I–I one it is 68.56 and 67.98 cm^{-1} for each PES.

Both surfaces predict the same ordering in the stability of the isomers, and their estimates for the binding energy of the conformers are in better agreement with experimental measurements available,[26,41] than with previous reported theoretical values.[24,27] By comparing the results of the two surfaces we found some quantitative differences on the energies of all bound states computed. For the higher lying vibrational levels, we show that the small differences in the representation of the potential energy surfaces of NeI_2 clearly affects the properties of these states of the system, not only quantitatively, but also qualitatively. As we discussed above our calculations indicate the coexistence of the two isomers for NeI_2 in a supersonic beam at very low temperatures. However, we should regard cautiously any relative ordering of the two isomers, as we found that their energy difference is very small within

the errors in the *ab initio* CCSD(T) calculations and in the representation of the PES. Therefore, given the difficulties of the previous experimental studies in determining equilibrium structures of different isomers,[26] further data, mainly experimental, on rovibrational bound states are needed for NeI_2 or similar clusters, in order to justify our assertions, and finally evaluate the present CCSD(T)/CBS[Q5] potentials.

ACKNOWLEDGMENTS

The authors thank Centro de Calculo (IFF), CTI (CSIC), and CESGA for allocation of computer time. This work has been supported by DGICYT, Spain, Grant No. FIS2010-18132.

[1] J. M. Pio, W. E. van der Veer, C. R. Bieler, and K. C. Janda, J. Chem. Phys. **128**, 134311 (2008).
[2] J. M. Pio, M. A. Taylor, W. E. van der Veer, C. R. Beiler, J. A. Cabrera, and K. C. Janda, J. Chem. Phys. **133**, 014305 (2010).
[3] D. S. Boucher, D. B. Strasfeld, R. A. Loomis, J. M. Herbert, S. E. Ray, and A. B. McCoy, J. Chem. Phys. **122**, 104312 (2005).
[4] S. E. Ray, A. B. McCoy, J. J. Glennon, J. P. Darr, E. J. Fesser, J. R. Lancaster, and R. A. Loomis, J. Chem. Phys. **125**, 164314 (2006).
[5] L. García-Gutierrez, L. Delgado-Tellez, A. Valdés, R. Prosmiti, P. Villarreal, and G. Delgado-Barrio, J. Phys. Chem. A **113**, 5754 (2009).
[6] A. Rohrbacher, N. Halberstadt, and K. C. Janda, Annu. Rev. Phys. Chem. **51**, 405 (2000).
[7] B. Lepetit, O. Roncero, A. A. Buchachenko, and N. Halberstadt, J. Chem. Phys. **116**, 8367 (2002).
[8] A. A. Buchachenko, R. Prosmiti, C. Cuhna, P. Villarreal, and G. Delgado-Barrio, J. Chem. Phys. **117**, 6117 (2002).
[9] R. Prosmiti, C. Cuhna, A. A. Buchachenko, G. Delgado-Barrio, and P. Villarreal, J. Chem. Phys. **117**, 10019 (2002).
[10] A. B. McCoy, J. P. Darr, D. S. Boucher, P. R. Winter, M. D. Bradke, and R. A. Loomis, J. Chem. Phys. **120**, 2677 (2004).
[11] R. Prosmiti, C. Cunha, P. Villarreal, and G. Delgado-Barrio, J. Chem. Phys. **117**, 7017 (2002).
[12] R. Prosmiti, C. Cunha, P. Villarreal, and G. Delgado-Barrio, J. Chem. Phys. **119**, 4216 (2003).
[13] A. Valdés, R. Prosmiti, P. Villarreal, and G. Delgado-Barrio, Chem. Phys. Lett. **375**, 328 (2003).
[14] M. P. de Lara-Castells, A. A. Buchachenko, G. Delgado-Barrio, and P. Villarreal, J. Chem. Phys. **120**, 2182 (2004).
[15] R. Hernández-Lamoneda and K. C. Janda, J. Chem. Phys. **123**, 161102 (2005).
[16] A. Valdés, R. Prosmiti, P. Villarreal, G. Delgado-Barrio, and H.-J. Werner, J. Chem. Phys. **126**, 204301 (2007).
[17] A. Valdés, R. Prosmiti, P. Villarreal, G. Delgado-Barrio, D. Lemoine, and B. Lepetit, J. Chem. Phys. **126**, 244314 (2007).
[18] S. M. Cybulski and J. S. Holt, J. Chem. Phys. **110**, 7745 (1999).
[19] R. Prosmiti, C. Cunha, P. Villareal, and G. Delgado-Barrio, J. Chem. Phys. **116**, 9249 (2002).
[20] R. Prosmiti, P. Villarreal, and G. Delgado-Barrio, Chem. Phys. Lett. **359**, 473 (2002).
[21] A. Valdés, R. Prosmiti, P. Villarreal, and G. Delgado-Barrio, Mol. Phys. **102**, 2277 (2004).
[22] D. B. Strasfeld, J. P. Darr, and R. A. Loomis, Chem. Phys. Lett. **397**, 116 (2004).
[23] R. Prosmiti, A. Valdés, P. Villarreal, and G. Delgado-Barrio, J. Phys. Chem. A **104**, 6065 (2004).
[24] S. Pakhira, B. Mondal, and A. K. Das, Chem. Phys. Lett. **505**, 81 (2011).
[25] J. A. Blazy, B. M. DeKoven, T. D. Russell, and D. H. Levy, J. Chem. Phys. **72**, 2439 (1980).
[26] A. Burroughs, G. Kerenskaya, and M. C. Heaven, J. Chem. Phys. **115**, 784 (2001).
[27] M. C. Heaven and A. A. Buchachenko, J. Mol. Spectrosc. **222**, 31 (2003).
[28] A. Valdés, R. Prosmiti, P. Villarreal, and G. Delgado-Barrio, J. Chem. Phys. **122**, 044305 (2005); **125**, 014313 (2006).
[29] M. P. de Lara-Castells, R. Prosmiti, G. Delgado-Barrio, D. López-Durán, P. Villarreal, F. A. Gianturco, and J. Jellinek, Phys. Rev. A **74**, 054611 (2006).
[30] C. Diez-Pardos, A. Valdés, R. Prosmiti, P. Villarreal, and G. Delgado-Barrio, Theor. Chem. Acc. **118**, 511 (2007).
[31] D. S. Boucher, J. P. Darr, D. B. Strasfeld, and R. A. Loomis, J. Phys. Chem. A **112**, 13393 (2008).
[32] A. Valdés, P. Barragán, R. P. de Tudela, L. Delgado-Tellez, J. S. Medina, and R. Prosmiti, "A theoretical characterization of multiple isomers of the He_2I_2 complex," Chem. Phys. (in press).
[33] MOLPRO, a package of *ab initio* programs designed by H.-J. Werner and P. J. Knowles, version 2009.1, M Schütz *et al.*; see http://www.molpro.net.
[34] S. F. Boys and F. Bernardi, Mol. Phys. **19**, 553 (1970).
[35] A. Bergner, M. Dolg, W. Kuechle, H. Stoll, and H. Preuss, Mol. Phys. **80**, 1431 (1993).
[36] M. Dolg, Habilitationsschrift, Universität Stuttgart (1997).
[37] J. M. L. Martin and A. Sundermann, J. Chem. Phys. **114**, 3408 (2001).
[38] K. A. Peterson, D. Figgen, E. Goll, H. Stoll, and M. Dolg, J. Chem. Phys. **119**, 11113 (2003).
[39] C. Schwartz, Phys. Rev. **126**, 1015 (1962).
[40] T.-S. Ho and H. Rabitz, J. Chem. Phys. **104**, 2584 (1996).
[41] R. A. Loomis, private communication (2005).